A Theoretical Study of Effect of Gate Voltage on Electron–Modulated-Acoustic-Phonon Interactions in Silicon Nanowire MOSFETs

Junichi Hattori*‡, Shigeyasu Uno*‡, Nobuya Mori†‡, and Kazuo Nakazato*
*Department of Electrical Engineering and Computer Science, Graduate School of Engineering, Nagoya University
Furo-cho, Chikusa-ku, Nagoya, Aichi 464-8603, Japan
Phone: +81-52-789-2794, Fax: +81-52-789-3139, E-mail: j_hattor@echo.nuee.nagoya-u.ac.jp, uno@nuee.nagoya-u.ac.jp
†Department of Electronic Engineering, Graduate School of Engineering, Osaka University
2-1 Yamada-oka, Suita, Osaka 565-0871, Japan
‡ JST, CREST 5 Sanbancho, Chiyoda-ku, Tokyo 102-0075, Japan

***Abstract*—We theoretically investigate the gate voltage dependence of the interaction between modulated acoustic phonons and electrons in SiO_2-coated Si nanowires. The gate voltage decreases the form factor calculated with modulated acoustic phonons as well as that for bulk phonons. However, the relative difference between the two form factors, that is, the phonon modulation effect on the form factor becomes larger with increasing gate voltage. In addition, we evaluate the phonon modulation effect on the electron mobility in the Si nanowires, and reveal that the effect becomes smaller with increasing gate voltage.**

***Index Terms*—acoustic phonon, electron-phonon interaction, electron mobility, Si nanowire, gate-all-around MOSFET**

I. Introduction

Silicon nanowire (SiNW) metal-oxide-semiconductor field-effect transistors (MOSFETs) have been attracting considerable attention as one of the promising device structure for further scaling of complementary metal-oxide-semiconductor owing to their excellent electrostatic gate control of the channel [1], [2]. Acoustic phonons in nanostructures are modulated by interfaces between acoustically different materials, and therefore they differ from bulk phonons. The impacts of such acoustic phonon modulation on electron transport in SiNWs have recently been assessed by comparison with the conventional bulk phonon model, and it has been revealed that the acoustic phonon limited electron scattering rate and mobility appreciably vary depending on the presence or absence of the modulation [3]–[9]. However, although the impacts also depend on electron states, it is not clear in operating SiNW MOSFETs how much effect the modification of electron states due to the gate voltage has on them. In this work, we theoretically investigate the interaction between modulated acoustic phonons and electrons in gate biased SiNWs.

II. Electron–Modulated-Acoustic-Phonon Interactions

We derived acoustic phonon and electron states in a cylindrical SiNW of radius a and infinite length coated with a SiO_2 shell of thickness t_{ox}, which is depicted in Fig. 1. Assuming the core and shell are isotropic continua, acoustic phonons can be described by Navier's equation. We solved the equation for two boundary conditions (BCs). One is that the shell surface is free. In such a free surface (FS) BC, the whole nanowire is assumed to be embedded in an extremely soft material such as a vacuum, and the stress vanishes at the shell surface. Another is the clamped surface (CS) BC, in which the nanowire is assumed to be embedded in an extremely hard material such as a rigid body and the phonon displacement becomes zero at the surface. The dispersion relations of acoustic phonons obtained for the two BCs are shown in Figs. 2(a) and 2(b). In the figures, the horizontal axes represent the phonon wavevector along the z-axis, q_z, multiplied by the core radius, a, and the vertical axes the frequency, ω, multiplied by a/v_{t}, where v_{t} is the transverse sound velocity in bulk Si. More information about acoustic phonons can be found in the literature [9].

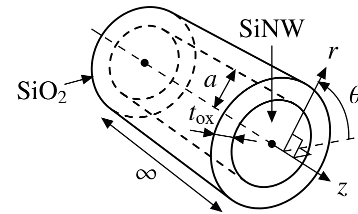

Fig. 1. Schematic view of the structure considered in this work.

The electron states, on the other hand, are described by the Schrödinger equation,

$$-\left[\frac{\hbar^2}{2m_r^*}\left(\frac{\partial^2}{\partial r^2}+\frac{1}{r}\frac{\partial}{\partial r}+\frac{1}{r^2}\frac{\partial^2}{\partial\theta^2}\right)+\frac{\hbar^2}{2m_z^*}\frac{\partial^2}{\partial z^2}\right]\Psi(\boldsymbol{r}) + V(\boldsymbol{r})\Psi(\boldsymbol{r}) = E\Psi(\boldsymbol{r}), \quad (1)$$

where $\Psi(\boldsymbol{r})$ is the electron wave function, m_r^* and m_z^* are the effective masses in the r- and z-directions, respectively, E is the energy, and $V(\boldsymbol{r})$ is the potential energy. Here, the electrons are assumed to have the isotropic mass, m_r^*, in the $r\theta$-plane [10]. With the assumption that the potential energy depends only on r, that is, $V(r,\theta,z)$ can be rewritten as $V(r)$, the energies and corresponding wave functions are given by

$$E_{mnk_z} = E_{mn} + E_{k_z} = E_{mn} + \hbar^2 k_z^2 \big/ 2m_z^*, \quad (2)$$

$$\Psi_{mnk_z}(r,\theta,z) = \psi_{mn}(r)\mathrm{e}^{\mathrm{i}(m\theta+k_z z)} \big/ \sqrt{2\pi L_z}, \quad (3)$$

where $m\ (=0,\pm1,\pm2,\dots)$ and $n\ (=1,2,3,\dots)$ are the electron confinement quantum numbers in the θ- and r-directions,

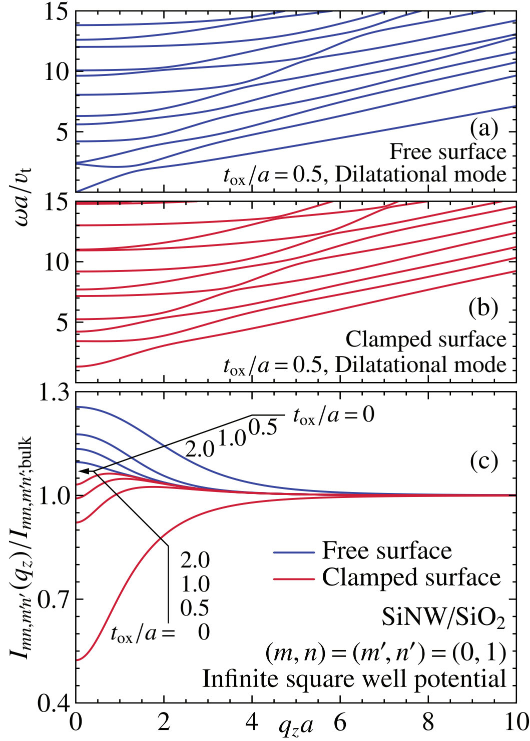

Fig. 2. (a), (b) Acoustic phonon dispersion relation of dilatational modes in a SiO_2-coated SiNW with a FS or CS. (c) Modulated phonon form factor as a function of $q_z a$ calculated for the intra-lowest-subband scattering and for different t_{ox}'s. The vertical axis is divided by the bulk phonon form factor.

respectively, k_z is the wavevector along the z-axis, E_{mn} is the confinement energy level in the $r\theta$-plane, E_{k_z} is the kinetic energy along the z-axis, $\psi_{mn}(r)$ is the radial dependence of the wave function, and L_z is the wire length. Furthermore, assuming $V(r)$ is given by the infinite square well potential of radius a, we can write E_{mn} and $\psi_{mn}(r)$ as

$$E^0_{mn} = \frac{\hbar^2}{2m^*_r}\left(\frac{j_{mn}}{a}\right)^2 \text{ and } \psi^0_{mn}(r) = \frac{\sqrt{2}}{aJ_{m+1}(j_{mn})}J_m\left(\frac{j_{mn}}{a}r\right),$$

respectively, where $J_m(r)$ are the Bessel functions of the first kind with order m and j_{mn} are their nth zeros.

Acoustic phonons scatter electrons through a deformation potential (DP), and the scattering rate can be written from Fermi's golden rule and the relaxation time approximation as

$$\frac{1}{\tau_{mn}(E_{k_z})} = \frac{n_v D^2_{ac} k_B T_L}{2\hbar^2 v_l^2 \rho}\sqrt{\frac{m^*_d}{2}} \sum_{m',n',\alpha,\beta}\left[I_{mn,m'n'}(q_z) \times \frac{1}{\sqrt{E_{k'_z}}}\left(1+\beta\sqrt{\frac{E_{k'_z}}{E_{k_z}}}\right)H(E_{k'_z})\right], \quad (4)$$

with $q_z = \alpha\sqrt{2m^*_c}\left(\sqrt{E_{k_z}} + \beta\sqrt{E_{k'_z}}\right)/\hbar$ and the electron kinetic energy along the z-axis after scattering, $E_{k'_z} = E_{mnk_z} - E_{m'n'}$. Here, n_v is the valley degeneracy with respect to intravalley scattering; D_{ac} is the acoustic DP constant in a SiNW; T_L is the lattice temperature; ρ is the mass density of Si; v_l is the longitudinal sound velocity in bulk Si; m^*_d and m^*_c are the electron density-of-states and conductivity masses, respectively, and they are equal to m^*_z; α takes values of either 1 or -1 for phonon emission or absorption; β takes values of either 1 or -1 for back or front scattering; $H(E)$ is the Heaviside step function. In addition, $I_{mn,m'n'}(q_z)$ is the form factor and represents the wave function overlap between electrons and acoustic phonons. For modulated acoustic phonons, the form factor is given by

$$I_{mn,m'n'}(q_z) = \frac{L_z\rho}{v_l^2}\sum_{q_l}\omega^2\left|\int_0^\infty \psi^*_{m'n'}(r)A_l J_{m'-m}(q_l r)\psi_{mn}(r)r\mathrm{d}r\right|^2, \quad (5)$$

where A_l is a quantity related to the phonon amplitude, and q_l is the longitudinal phonon wavevector in the r-direction. On the other hand, for bulk phonons the form factor is given by

$$I_{mn,m'n';\mathrm{bulk}} = \frac{1}{2\pi}\int_0^\infty\left|\int_0^\infty \psi^*_{m'n'}(r)J_{m'-m}(q_r r)\psi_{mn}(r)r\mathrm{d}r\right|^2 q_r\mathrm{d}q_r, \quad (6)$$

which depends only on the radial dependence of the initial and final electron wave functions. Using the scattering rate given by (4), we can write the electron mobility as

$$\mu_{mn} = \frac{2e}{m^*_c}\int_0^\infty \tau_{mn}(E_{k_z})\sqrt{E_{k_z}}\left[-\frac{\partial f(E_{mnk_z}, E_F)}{\partial E_{k_z}}\right]\mathrm{d}E_{k_z} \times \left[\int_0^\infty \frac{1}{\sqrt{E_{k_z}}} f(E_{mnk_z}, E_F)\mathrm{d}E_{k_z}\right]^{-1}, \quad (7)$$

where E_F is the Fermi energy and $f(E, E_F)$ is the Fermi–Dirac distribution. In the above electron scattering rate and mobility, the differences between modulated and bulk phonons appear only through the form factor. Thus, the form factor is the most fundamental quantity representing the impacts of acoustic phonon modulation on electron transport.

Figure 2(c) shows the form factor for the intra-lowest-subband scattering mediated by modulated acoustic phonons in SiO_2-coated SiNWs. In the calculation, the electron states in the infinite square well potential were used. This figure also shows the results for bare SiNWs. The form factor for a bare SiNW having a FS is always larger than that for bulk phonons, because the FS allows phonons to vibrate more freely than those in a Si-coated SiNW or bulk Si. This form factor increase enhances the electron scattering and degrades the mobility as shown in Fig. 3 by the blue dashed line. On the other hand, the form factor for a bare SiNW with a CS is always smaller than the bulk phonon form factor. This is because the CS prohibits phonons from vibrating on the surface and consequently the phonon waves within the SiNW becomes weaker. As a result, the electron transport properties improve, which is shown in Fig. 3 by the red dashed line. The results for SiNWs coated with SiO_2 shells have values intermediate between the two extreme cases. The thicker the shell becomes, the smaller the influence of its surface becomes, and accordingly the form factor approaches a certain line regardless of the BC, as can be seen in Fig. 2(c). The line shows exactly the effects of acoustic phonon modulation due to the interface between a SiNW and a SiO_2 shell, and resembles that for a free-standing

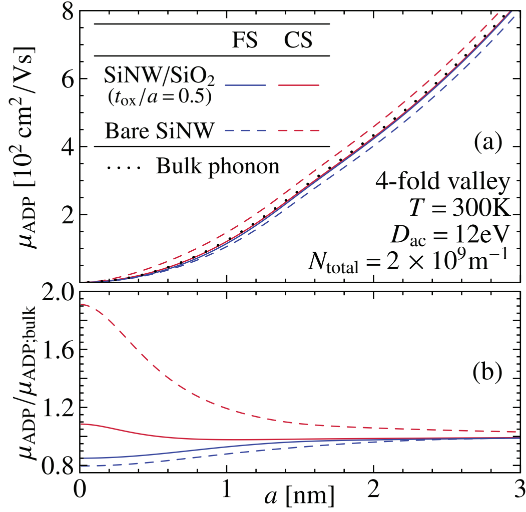

Fig. 3. (a) Modulated acoustic phonon limited electron mobility for the 4-fold valley in [001]-oriented SiNWs, plotted as a function of a. (b) Its ratio to the bulk phonon limited mobility. In the calculation, it was assumed that all electrons exists only in the lowest subband of each valley.

SiNW to some extent since SiO_2 is acoustically softer than Si. The acoustic hardness of material is expressed by the acoustic impedance, which is defined as ρv_l or ρv_t. If the shell is acoustically harder than the core and sufficiently thick, the form factor would be smaller than that for bulk phonons, and the electron transport properties would improve [9], as in the case of a bare SiNW with a CS.

III. Effects of Gate Voltage

All calculations in the previous section were done for electrons confined to the infinite potential well having a flat bottom. In SiNW MOSFETs, however, the potential is not flat, but bent due to the gate voltage. To take into account such potential bending, we solved the Schrödinger equation (1) with the potential energy, $V(r) = V^0(r) - e\phi(r)$, where $V^0(r)$ is the infinite square well potential of radius a, and $\phi(r)$ is the electrostatic potential in a cross section of the nanowire and is obtained from the Poisson equation,

$$\left(\frac{1}{r}\frac{\mathrm{d}}{\mathrm{d}r} + \frac{\mathrm{d}^2}{\mathrm{d}r^2}\right)\phi(r) = \frac{eN_\mathrm{total}(r)}{\varepsilon_\mathrm{ch}}. \tag{8}$$

Here, ε_ch is the permittivity of the core, and $N_\mathrm{total}(r)$ is the electron density per unit volume, which is given by

$$N_\mathrm{total}(r) = \sum_{v,m,n}\left[|\psi_{mn;v}(r)|^2 \frac{1}{\pi^2\hbar}\sqrt{\frac{m^*_{\mathrm{d};v}}{2}} \times \int_0^\infty \frac{1}{\sqrt{E_{k_z;v}}} f(E_{mnk_z;v}, E_\mathrm{F})\mathrm{d}E_{k_z;v}\right], \tag{9}$$

where v denotes the vth conduction band valley. We introduced the technique presented in the literature [11] to solve (1) with the new potential energy. Although we have to solve (1) and (8) self-consistently, for this purpose we used the scheme presented in the literature [12].

Figure 4 shows the gate voltage dependence of the electron states in a [001]-oriented SiNW of $a = 2$ nm coated with a

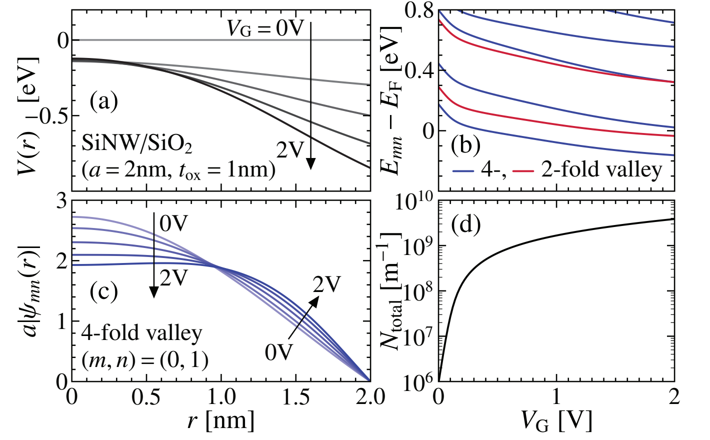

Fig. 4. Electron states in a cross section of a [001]-oriented SiNW coated with a SiO_2 shell under different gate voltages: (a) potential energy; (b) energy levels measured from E_F; (c) wave function for the lowest subband in the 4-fold valley; (d) density per unit length.

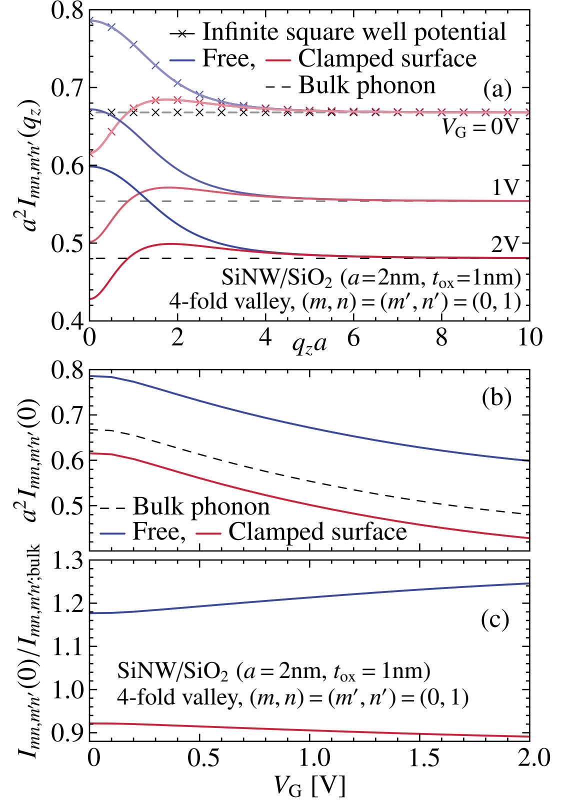

Fig. 5. (a) Modulated and bulk phonon form factors as a function of $q_z a$ calculated for several V_G's. (b) The two form factors at $q_z a = 0$ plotted as a function of V_G. (c) Their ratio.

SiO_2 shell of $t_\mathrm{ox} = 1$ nm. In the calculation, it was assumed that $E_\mathrm{F} = 0$ eV and the affinity in the core is equal to the work function in the gate metal, so that the flat band voltage is 0 V. Using the obtained electron wave functions, we calculated the modulated and bulk phonon form factors for the intra-lowest-subband scattering in the 4-fold valley, which are shown in Fig. 5(a). At $V_\mathrm{G} = 0$ V, the two form factors are identical to those calculated with the infinite square well potential, because the potential energy is almost flat. With increasing V_G, however, they become smaller, which is clearly

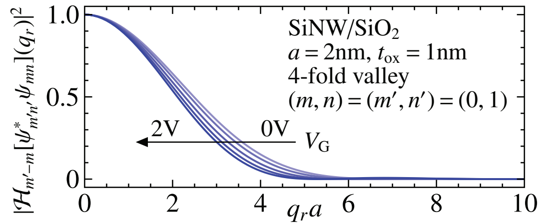

Fig. 6. Radial wavevector spectrum of the product of the initial and final wave functions for the intra-lowest-subband scattering, which can be obtained from the Hankel transform, $\mathcal{H}_m[f](q_r) = \int f(r)J_m(q_r r)r\mathrm{d}r$.

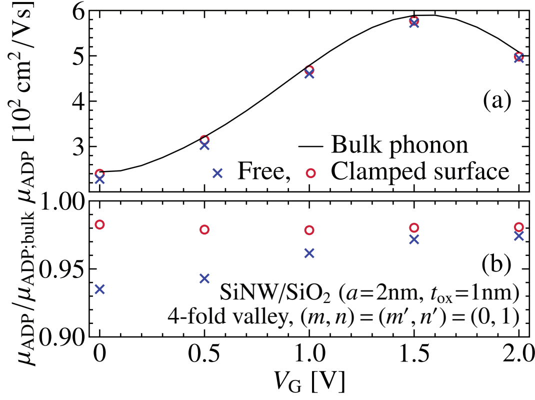

Fig. 7. (a) Modulated phonon limited electron mobility in the lowest subband calculated for several V_G's. (b) Its ratio to the bulk phonon limited mobility. In the calculation, the acoustic phonon modulation was taken into account only for the intra-lowest-subband scattering.

seen in Fig. 5(b). The figure shows the two form factors at $q_z a = 0$ as a function of V_G. As can be seen in Fig. 4(c), the electron wave function spreads throughout the cross section with increasing V_G, and accordingly it becomes narrower in the radial wavevector domain. The radial wavevector spectrum of the product of the initial and final wave functions for a scattering, which is shown in (5) and (6) as the radial integral with $A_l = 1$, shows the contribution of individual acoustic phonon modes to the scattering. The spectrum for the intra-lowest-subband scattering is shown in Fig. 6, and as expected, it narrows toward small wavevector with increasing V_G, which indicates that phonons with a relatively large wavevector become less able to contribute to the scattering. Thus, the form factor decreases whether with or without acoustic phonon modulation. Figure 5(c) shows the ratio of the two form factors at $q_z a = 0$. This figure indicates that with increasing V_G the modulated phonon form factor for the FS BC becomes larger than the bulk phonon form factor at $q_z a = 0$, while that for the CS BC becomes smaller. In other words, a larger V_G enhances the acoustic phonon modulation effects. This is because the wave function becomes closer to the interface between the core and shell which causes phonon modulation. Similar behavior of the form factor as described above has been observed for several SiO_2-coated SiNWs with different core radii and shell thicknesses.

Figure 7 shows the electron mobility calculated for the lowest subband in the 4-fold valley with the form factors shown in Fig. 5(a). The form factor reduction due to the gate voltage leads to better mobility. According to (7), the electrons with energy around E_F determine the mobility since the derivative of $f(E, E_F)$ has its peak at $E = E_F$. As can be seen in Fig. 4(b), such major electrons in the lowest subband have larger kinetic energy, E_{k_z}, with increasing V_G. Their scattering rate given by (4) accordingly becomes smaller because the intra-lowest-subband scattering rate decreases inversely with $\sqrt{E_{k_z}}$. This is another and decisive reason why the mobility increases in the region of low and moderate V_G, However, V_G becomes larger than about 1.5 V, the mobility degrades. This is because some of the major electrons have energy slightly larger than the first excited level, and they come across the spike of the scattering rate from the lowest to the first excited subband, which arises from the term, $1/\sqrt{E_{k'_z}}$, in (4). As for the phonon modulation effects, under the FS BC the mobility limited by modulated phonons approaches that for bulk phonons with increasing V_G. This is because the wavevector of phonons which scatter the electrons determining the mobility increases according to $|q_z| = 2\sqrt{2m^*_c E_{k_z}}/\hbar$, and the modulated phonon form factor at larger $|q_z|$ becomes closer to the bulk phonon form factor as can be seen in Fig. 5(a). Under the CS BC, on the other hand, the mobility is almost equal to that for bulk phonons and their ratio varies little with V_G. As seen in Fig. 5(a), the form factor for the CS BC has the two regions where its value is obviously larger or smaller than the bulk phonon form factor. Although the influences of the two regions on the mobility differ from each other, they are almost equally weighted by the derivative of $f(E, E_F)$ and then integrated in (7) because the two regions lie next to each other. As a result, their influences are canceled out, and therefore the resulting mobility has almost the same value as the bulk phonon limited mobility for any V_G.

IV. Conclusion

The gate voltage dependence of the interaction between modulated acoustic phonons and electrons in SiO_2-coated SiNWs was investigated theoretically. It was found that the gate voltage decreases the modulated phonon form factor as well as the bulk phonon form factor. The relative difference between the two form factor, however, becomes larger with increasing gate voltage. In addition, the electron mobility in the SiNWs was calculated. In contrast to the case of the form factor, the phonon modulation effect on the mobility becomes smaller with increasing gate voltage.

References

[1] N. Singh *et al.*, *IEEE Electron Device Lett.*, vol. 27, pp. 383–386, 2006.
[2] K. H. Yeo *et al.*, IEDM Tech. Dig., 2006, pp. 539–542.
[3] V. A. Fonoberov and A. A. Balandin, *Nano Lett.*, vol. 6, pp. 2442–2446, 2006.
[4] A. K. Buin *et al.*, *Nano Lett.*, vol. 8, pp. 760–765, 2008.
[5] ——, *J. Appl. Phys.*, vol. 104, p. 053716, 2008.
[6] E. B. Ramayya *et al.*, *J. Comput. Electron.*, vol. 7, pp. 319–323, 2008.
[7] ——, *J. Appl. Phys.*, vol. 104, p. 063711, 2008.
[8] J. Hattori *et al.*, *J. Appl. Phys.*, vol. 107, p. 033712, 2010.
[9] ——, *Jpn. J. Appl. Phys.*, vol. 49, p. 04DN09, 2010.
[10] E. Gnani *et al.*, *IEEE Trans. Electron Devices*, vol. 54, pp. 2243–2254, 2007.
[11] ——, Proc. ESSDERC, 2004, pp. 177–180.
[12] A. Trellakis *et al.*, *J. Appl. Phys.*, vol. 81, pp. 7880–7884, 1997.